The Effects of Water on Blast

From the Simultaneous Detonation of 180

152 mm Shells

by

Joseph Crepeau
and
Charles Needham

Applied Research Associates, Inc.
4200 San Mateo Blvd. NE
Albuquerque, NM 87110

Presented at the

Twenty-Eighth DoD Explosives Safety Seminar
18-20 August 1998
Orlando, Florida, USA

Report Documentation Page

Form Approved
OMB No. 0704-0188

1. REPORT DATE **AUG 1998**	2. REPORT TYPE	3. DATES COVERED **00-00-1998 to 00-00-1998**

4. TITLE AND SUBTITLE **The Effects of Water on Blast From the Simultaneous Detonation of 180 152 mm Shells**	5a. CONTRACT NUMBER 5b. GRANT NUMBER 5c. PROGRAM ELEMENT NUMBER
6. AUTHOR(S)	5d. PROJECT NUMBER 5e. TASK NUMBER 5f. WORK UNIT NUMBER
7. PERFORMING ORGANIZATION NAME(S) AND ADDRESS(ES) **Applied Research Associates, Inc,4200 San Mateo Blvd. NE,Albuquerque,NM,87110**	8. PERFORMING ORGANIZATION REPORT NUMBER
9. SPONSORING/MONITORING AGENCY NAME(S) AND ADDRESS(ES)	10. SPONSOR/MONITOR'S ACRONYM(S) 11. SPONSOR/MONITOR'S REPORT NUMBER(S)

12. DISTRIBUTION/AVAILABILITY STATEMENT
Approved for public release; distribution unlimited

13. SUPPLEMENTARY NOTES
See also ADM001002. Proceedings of the Twenty-Eighth DoD Explosives Safety Seminar Held in Orlando, FL on 18-20 August 1998.

14. ABSTRACT
see report

15. SUBJECT TERMS

16. SECURITY CLASSIFICATION OF:			17. LIMITATION OF ABSTRACT	18. NUMBER OF PAGES	19a. NAME OF RESPONSIBLE PERSON
a. REPORT **unclassified**	b. ABSTRACT **unclassified**	c. THIS PAGE **unclassified**	**Same as Report (SAR)**	**17**	

1. Abstract

ARA was asked and funded by the Naval Facilities Engineering Service Center (NFESC) to perform calculations of the airblast resulting from the simultaneous detonation of 180 six inch (152 mm) naval artillery shells. The calculations were run within the geometry of the KLOTZ Club tunnel test site at Alvdalen, Sweden. This geometry includes two crossing tunnels with a chamber at the end of each and a single tunnel entrance. A berm was constructed just outside the tunnel entrance to provide absorption and deflection of fragments. A test was conducted at this facility with 180 six-inch shells in 1989. In September of 1996 this test was repeated with 2000 kg of water in the vicinity of the detonation. Results of the two tests showed some surprises such as higher pressures near the tunnel entrance when water was present.

ARA was asked to make detailed first principles calculations that included the effects of water on the airblast. SHAMRC was used to make several three dimensional calculations of the two tests. SHAMRC includes the detonation process, the effects of accelerating, heating and vaporizing the water and propagation of the resulting airblast. Previous experience at Alvdalen, Sweden and at Magdalena, New Mexico had shown us that the response of the walls of the detonation chamber could be an important energy absorbing mechanism for large charges but was ignored for this relatively small loading density.

The initial conditions for the calculations used two planes of symmetry through the charge, thus the detonation of the explosive in an equivalent of only 45 shells (245 kg.) was calculated. A bare charge calculation was run which ignored the effects of the steel casing of each shell. This calculation included three materials: air, detonation products, and solid explosive. The results of this calculation provide the initial conditions for a series of calculations that included increasingly larger portions of the tunnel system. A second calculational series included the water in the airblast mitigation system. A third calculational series modeled the individual shells, including the steel casing, but without the water, to determine the effects of the charge models on the resultant airblast.

Each of the calculational series was run to a time at which the airblast had exited the tunnel system. Comparisons of the calculational results are made with available experimental data. Comparisons were also made between the calculations with the two charge models.

2. Introduction

The Naval Facilities Engineering Service Center (NFESC) has tasked Applied Research Associates (ARA) to perform three-dimensional (3D) hydrodynamic computer calculations of the full-scale tests conducted in the KLOTZ-club tunnel in Alvdalen. The tests were sponsored by the KLOTZ-club and Singapore in an effort to determine the effects of water on the mitigation of airblast effects from the detonation of munitions stored in a large tunnel system. The calculations were run using SHAMRC (Second-order Hydrodynamic Automatic Mesh Refinement Code, pronounced “shamrock”). Three series of calculations were made. The first series of calculations did not include the effects of water and used a bare TNT charge to model the shells. The second series used the same charge and modeled the water containers placed around the charge in the test performed in 1996. The third series of calculations modeled the

individual shells (the HE and the steel casing) during the detonation. At later times, the steel from the shell casings was removed from the calculation and replaced with massive, interactive particles.

The experiments conducted at Alvdalen have resulted in pressure and debris data that are difficult to understand and interpret. When water was added in the vicinity of the charge, pressures were reduced in the tunnel system but greater pressures were measured outside the tunnel. The purpose of these calculations is to determine if the experiment can be accurately modeled by computer calculations. If so, the calculations can be used to determine the cause for the unexpected behavior outside the tunnel system.

3. Calculational Initial Conditions

Because of the geometry of the experimental setup, all calculations were run in 3D in several stages. The first stage was the detonation of the charge. This calculation was carried out until the entire charge was completely detonated. The results of the detonation calculation were mapped into the larger grid of the second stage calculation, which comprised Chamber A of the tunnel system. This calculation was run until shock arrival at the transition region between Chamber A and the main tunnel. Results of that calculation were then mapped into the third stage, which contained Chamber A, a portion of the main tunnel, Chamber B and the cross tunnel. The fourth and final stage of the calculation included the entire tunnel system and a small portion of the region outside the tunnel entrance. Figure 1 is a plan view of the entire tunnel system.

At each stage transition, the zoning in the calculation was adjusted to cover the region of interest with zoning that was fine enough to capture the important shock interactions but not too fine that the calculation was prohibitively expensive to run. The setup of each stage also took advantage of the inherent symmetry of the calculated region. The detonation calculation required only one quarter of the charge to be calculated due to the symmetry of the charge.

Several stations were placed throughout the tunnel system to record parameter versus time information from the calculations. The majority of the stations were placed in Chamber A and the main tunnel. Stations were placed at multiple heights and locations across the tunnel width as well as several distances down the length of the main tunnel. Stations were also placed at locations that corresponded to experimental gage positions so that direct waveform comparisons could be made. The calculations were all run at ambient sea-level conditions ($P = 1.01302e6$ dynes/sq.-cm, $I = 2.044e9$ ergs/gm and $\rho = 1.225e-3$ gm/cc).

3.1 Bare Charge Without Water

In the detonation calculation, one-centimeter zones were used in all three dimensions of the calculational grid for a total of 2.5 million zones. When the detonation calculation was mapped into the second stage calculation (at a time of 100 μs), one half of chamber A was modeled with the plane of symmetry running down the centerline of the chamber. The zone size was increased to 2 cm in each dimension. The grid for this calculation required a total of 23.5 million zones. The results of the detonation calculation were mapped into the grid and reflected about the charge center. The remaining two stages of the calculations were run without a plane of

symmetry. The results of the second stage were mapped into the third stage calculation at a time of 4.5 ms. The zones were doubled in size to 4 cm resulting in a total of 18.6 million zones. The final stage calculation, which includes the entire tunnel system, kept the minimum zone size at 4 cm but moved these small zones into the main tunnel region from the tunnel entrance to the beginning of Chamber A. Because the region of interest was the main tunnel, Chamber A and the region directly outside the tunnel entrance used expanding zones. Fairly large zones were also used in the side tunnels and chamber B. The results from the third stage calculation were mapped into this calculation at 14 ms. Figure 2 is a 3D view of the entire tunnel system as modeled in this calculation. This same model was used for the other two calculational series.

In the experiment, the charge consisted of 180, 15.2-cm artillery shells stacked on pallets in the center of chamber A. The total weight of each shell was 44.6 kg with 5.45 kg of that mass being TNT. Thus the total weight of TNT was approximately 981 kg. The shells were detonated individually and simultaneously at the top of the shell. The first and second calculational series modeled the charge as a solid block of TNT whose dimensions of 100 cm wide by 160 cm long by 39.3 cm in height roughly approximated the dimensions of the stacked shells and whose total mass was 983 kg. The calculation used a loading density of 1.56 gm/cc and a detonation energy of 4.3e10 ergs/gm for the TNT. Figure 3 is a representation of the charge as modeled in these calculations. The block of TNT was detonated with a planar detonation region at the top of the block. This simplification of the charge was used to make the setup of the calculation simpler. Both the unmitigated and water mitigated calculation were run using this simplified charge model. It was felt that since the main purpose of the calculations was to determine the effects of the water on the resultant airblast that the charge simplification would not affect these results.

3.2 Steel Cased Charge Without Water

The detonation calculation that modeled the individual shells required almost 32 million zones with a zone size of 0.5 cm in each dimension. The smaller zones were required to resolve the shell casing properly. Figure 4 shows the individual shells (one quarter of them) as modeled in this calculation. This calculation, which took much longer to run, was setup and run while the other stages using the simplified charge model were being run. The results of this calculation were mapped into the second stage calculational grid at 120 μs. Succeeding calculations in this series used the same grid setups as the bare charge calculations so that the effects of the casing on the resultant airblast could be determined.

3.3 Bare Charge With Water

The calculational series containing water used the same bare charge detonation calculation as the series without water. The detonation calculation was mapped into the calculational grid at a time prior to the airblast interacting with the water (100 μs). The experiment used water containers placed in close proximity to the charge. The calculation modeled this by placing water in zones near the charge. The mass of the containers was felt to be unimportant and was ignored. Figure 5 is a representation of the calculational setup with the water. The water was placed on all four sides of the charge in regions that closely approximated those occupied by the water containers in the experiment. The water regions at the ends of the charge (down the length of the chamber) were 120 cm wide by 60 cm deep by 52 cm high. The water regions on the sides of the charge were 240 cm long (down the length of the chamber) by 50 cm deep by 52 cm high. The water on

all four sides of the charge was placed 90 cm from the edge of the charge. The total amount of water modeled in the calculation was 1980 kg.

4. Calculational Results

4.1 Bare Charge Without Water

Figure 6 shows the bare charge results at 1 ms, just after the detonation is complete. This is a slice through the calculation at a height of 1 meter above the floor. The upward moving shock is near the roof of the chamber and a shock reflected from the walls is traversing the detonation products. The shock is still 7 meters from the back wall of the detonation chamber.

By a time of 13 ms (Figure 7) the shock has propagated nearly 50 meters along the tunnel. The shock is beginning to propagate into the side tunnel and into chamber B. Strong secondary shocks can be seen in the detonation chamber.

4.2 Steel Cased Charge Without Water

Because the steel mass was in excess of 7000 kg, the effect of the steel on the blast wave was profound. More than half of the detonation energy was converted to kinetic energy of the steel fragments. Because of the relatively short distance from the detonation to the wall, very little of the kinetic energy of the fragments was converted back to internal energy of the gas. Thus over half of the detonation energy was lost to the flow and absorbed in the walls.

Figure 8 shows a horizontal slice through the detonation chamber at a time of 1 ms. The influence of the steel casings of each individual shell can be seen. The shock has just reached the walls of the detonation chamber. The reduced energy of the shock slows its propagation. Figure 9 shows the shocks at about the same location as that of the bare charge in Figure 7. The shock has taken nearly twice as long to reach the tunnel intersection as for the bare charge. The peak pressure is less than one third of that of the uncased charge.

4.3 Bare Charge With Water

The density in Figure 10 is dominated by the water. At a time of 1 ms most of the water is still at full ambient density of 1.0. The shock has traveled through and around the water but has moved the water only a few centimeters. The shock does not reflect as strongly from the detonation chamber walls as it did without the water.

The propagation velocity of the shock through the tunnel system is only marginally slower than for the bare charge without water. The shock for this case is at the same location as the bare charge at a time of 14 ms (Figure 11); only 1 ms longer than the bare charge.

4.4 Arrival time comparisons

Figure 12 compares the arrival times for the primary shock for each of the three calculations. The effect of the 7 tons of steel can be seen at a distance of less than 20 meters from the charge center, just outside the detonation chamber. The shock takes nearly twice as long to exit the

detonation chamber as the bare charge. The presence of water has little effect on the arrival time at the exit of the detonation chamber.

As the shocks continue to propagate through the tunnel system, the steel cased charge falls further behind the uncased charges, remaining a factor of two slower at all ranges. The presence of water only marginally slows the shock.

4.5 Peak Overpressure comparisons

Figure 13 shows a comparison of the peak overpressure as a function of distance from the charge for the three calculations. The bare charge with no water gives the highest pressures at all ranges beyond 20 meters. The steel cased charge falls approximately a factor of three lower than the bare charge at all ranges. The addition of water actually increased the pressure in the detonation chamber and near the exit of the detonation chamber. As the shock continued to propagate in the tunnel system, the water reduces the pressure for most of the distances by about 25%. A secondary signal catches the front near the 60-meter range.

4.6 Pressure Waveform Comparisons

At a distance of 50 meters from the entrance, about 35 meters from the charge, the waveforms from the three calculations are compared in Figure 14. The peak pressure from the bare charge is in excess of 40 bars. The presence of water reduced the peak to about 30 bars. The secondary shock in the bare charge calculation is nearly 25 bars but was reduced to about 15 bars when the water was present. The secondary peak is the reflected shock from the back of the detonation chamber. This second shock traversed approximately three times as much water as the primary shock exiting the detonation chamber. This probably explains the significant reduction. The steel casing reduced the first peak pressure to about 12 bars but the secondary peak is almost as large as the first at 10 bars.

The waveforms at a distance of 25 meters from the tunnel entrance are compared in Figure 15. The bare charges with or without water are in excess of 26 bars. The water reduced the second peak from 22 bars to 12 bars and delayed the secondary arrival by about 20 ms. The steel cased charge arrives over 20 ms later than the bare charge and has a peak of about 8 bars and a secondary peak of about 7 bars.

At a distance only 2.5 meters (Figure 16) from the tunnel entrance, the second peak from the bare charge is greater than the first and has nearly caught the primary shock. The water continues to hold down the second peak in that case and shows a second peak reduced by about 30% from the primary shock front. The first and second peaks from the steel cased detonation are nearly equal in magnitude and are 25 to 30 percent of the peaks produced by the uncased charges.

5. Comparisons With Experimental Data

The experimental waveform data is compared in Figure 17 with the waveform from the calculation with the steel casing, without water. The experimental data show an impulse enhancement at measuring point 16 of more than 20 percent when water is present. The

difference in impulse is due almost entirely to the late time enhancement in the pressure waveform.

The effects of water on the airblast can be obtained by comparing the results of the two bare charge calculations and by comparing the experimental data for the two conditions. The bare charge calculations show about a 10 % reduction in peak overpressure but a significant reduction in the second peak and a reduction in the late time pressure when water is present (Figure 14). The calculations also show about a 20% reduction in impulse.

The experimental data show nearly identical overpressure waveforms (Figure 18) at measuring point 15 (25 meters from the entrance) with a difference of less than 10 percent in impulse. The calculations at this location (Figure 15) show less than a 10 % difference in peak pressure, a reduction in pressure during and immediately after the second peak returning to agreement at late time. The result is an overall reduction in impulse of about 20 %.

At the tunnel exit, a distance of 2.5 meters inside the tunnel, the experimental peak pressure is reduced by about 20% (Figure 19). The impulse from the case with water is about 25% less than the case without water. The calculations at this position (Figure 16) show a reduction in first peak pressure of 10 % and a significant reduction in the second peak pressure from 23 bars to 11 bars. The resulting impulse is reduced by 20% when the water is present.

6. Conclusions

Three calculations were completed and compared with each other and with the experimental data. Of the three calculations the best direct agreement with experimental waveform data was obtained from the calculation which included the mass of the steel shell casings. The waveforms obtained at the exit of the detonation chamber show agreement in peak overpressure and time between arrival of the first and second peaks. As the shock travels down the tunnel from the detonation chamber, the calculated peaks are significantly greater than the measured values. Previous two-dimensional calculations have demonstrated the importance of tunnel wall roughness in decreasing the peak pressure as a function of distance. Tunnel wall roughness was not included in these three dimensional calculations.

The waveforms near the tunnel exit have the greatest impact on the exterior pressure propagation. The calculational results and the experimental results near the tunnel opening show that the pressure and impulse are reduced when water was used. The reductions are the order of 20 to 25 % from either the calculations or the experimental data. The primary loss of impulse is from a region near and after the second peak arrival. The second peak is the reflection from the back of the detonation chamber and has traversed the greatest distance through the region effected by water. At later times the waveforms from the calculations and experiments merge and are in agreement.

The presence of the steel casing material must be taken into account. More than half the detonation energy is converted into kinetic energy of the steel fragments. This loss of energy reduces the air blast energy by more than a factor of 2. The direct result of this energy loss is a reduction in blast impulse of nearly a factor of 3. The remainder of the total energy is retained in the hot gasses in the detonation chamber.

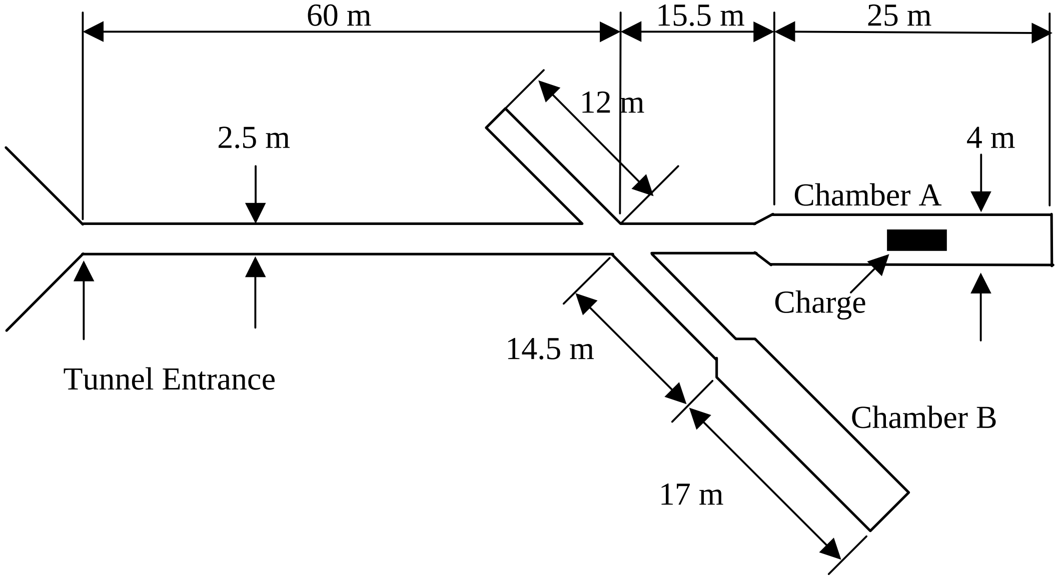

Figure 1 Plan View of Tunnel System as Modeled in Calculations

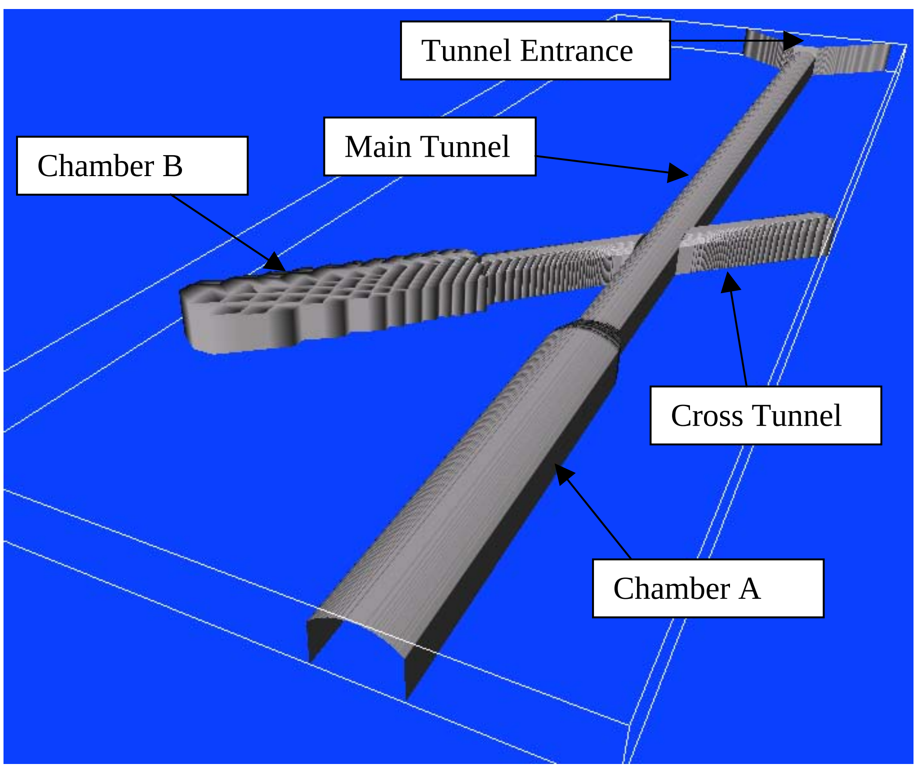

Figure 2 3D Tunnel System Model

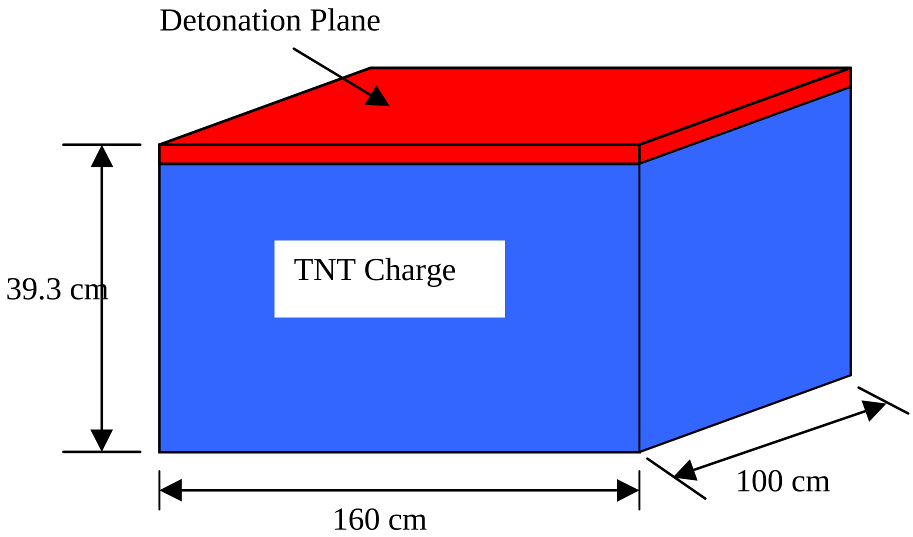

Figure 3 TNT Charge as Modeled in Calculations

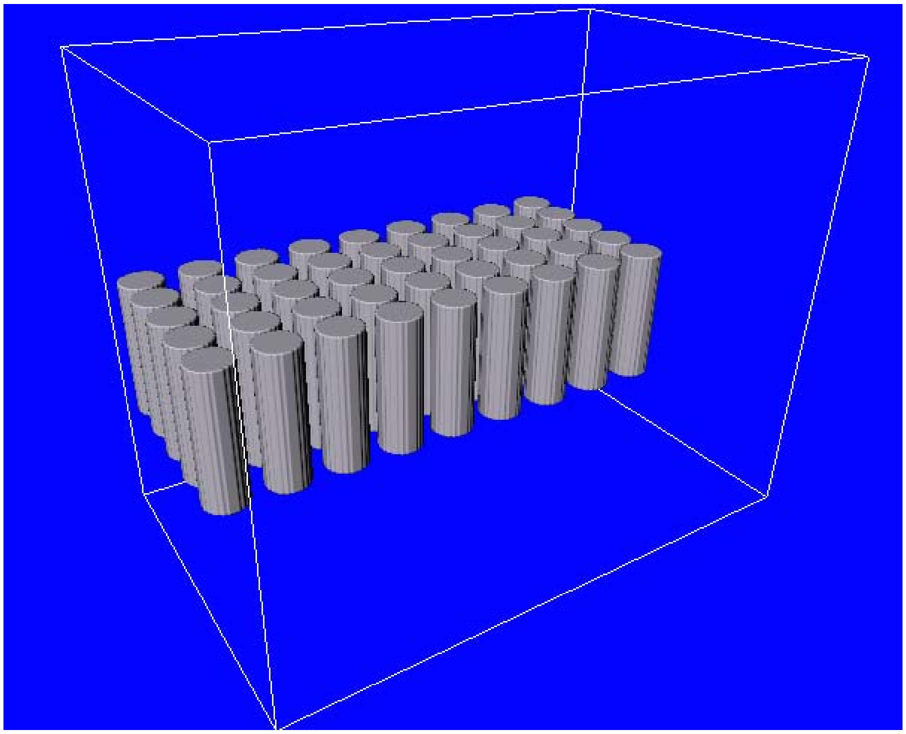

Figure 4 Model With Individual Shells

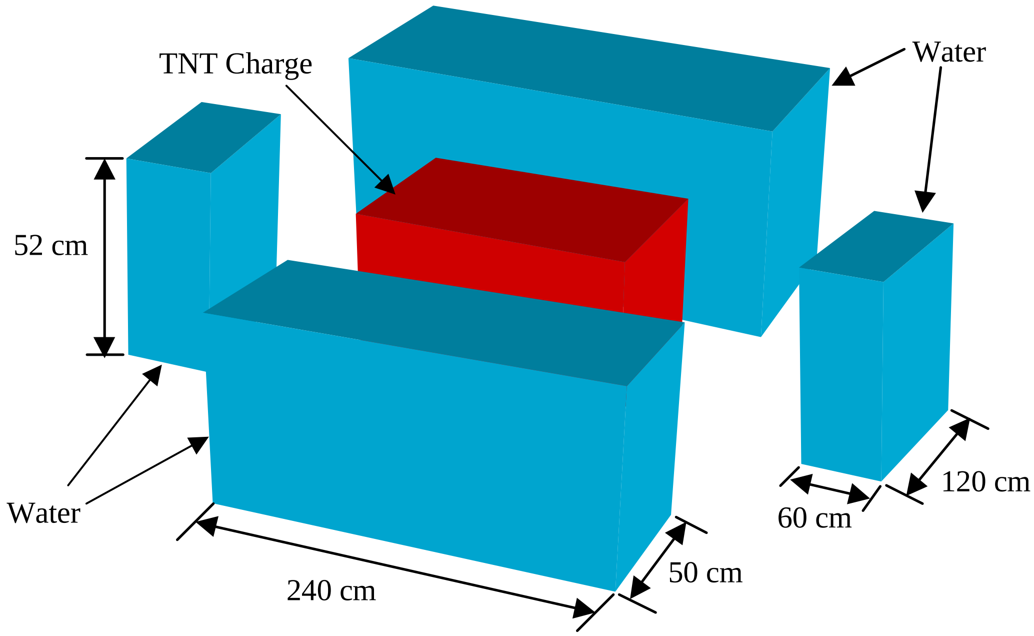

Figure 5 Setup for Water Calculation

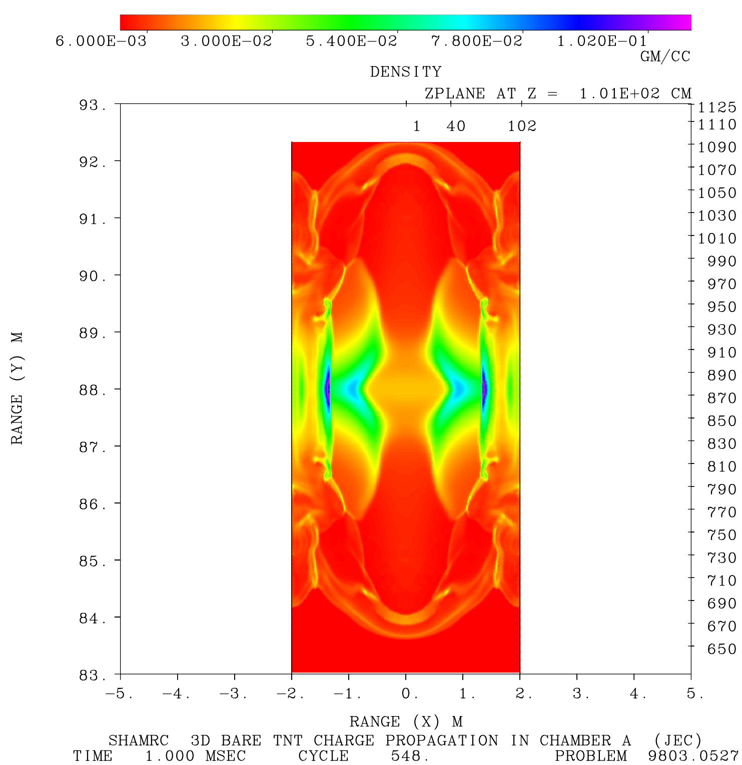

Figure 6 Density at 1ms From Bare Charge Without Water

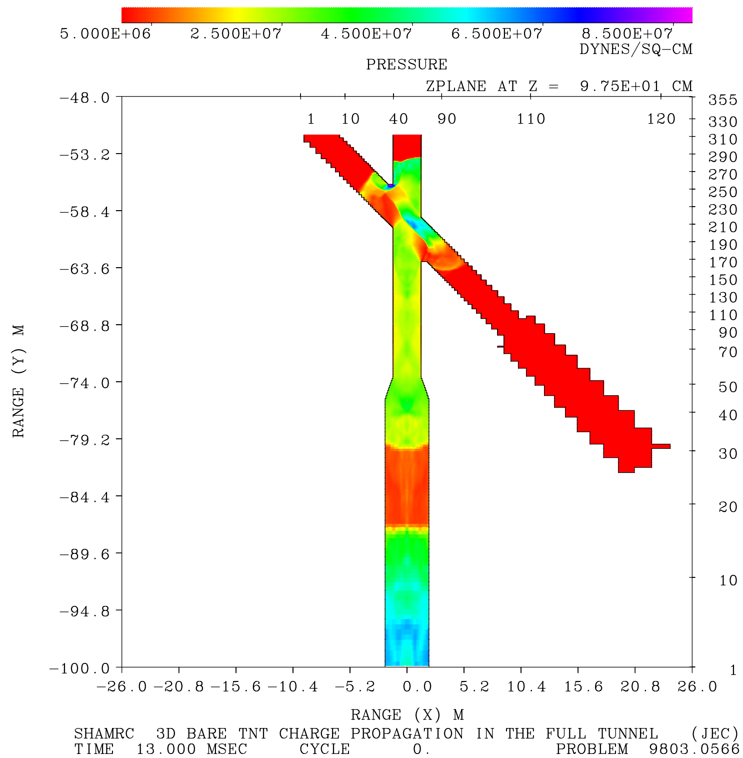

Figure 7 Pressure at 13 ms From Bare Charge Without Water

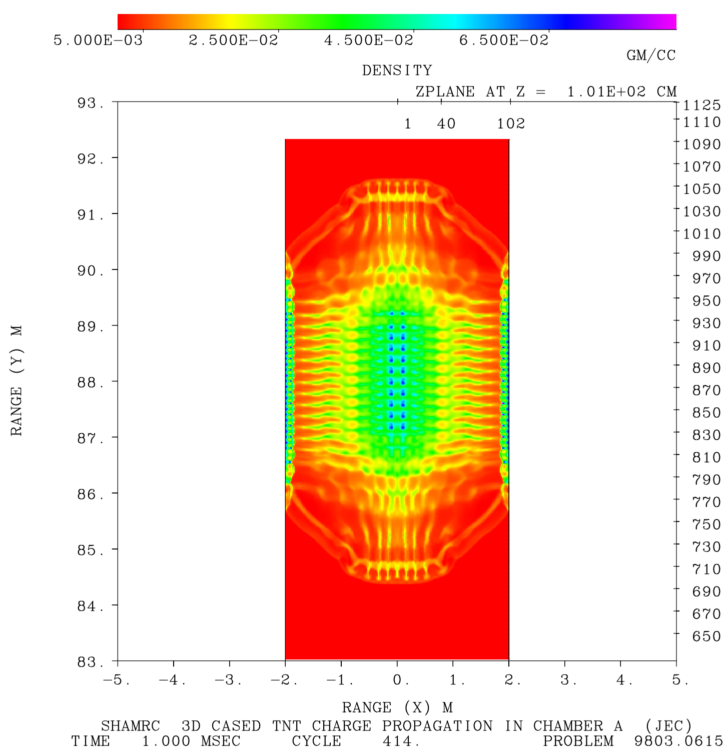

Figure 8 Density at 1 ms From Cased Charge Without Water

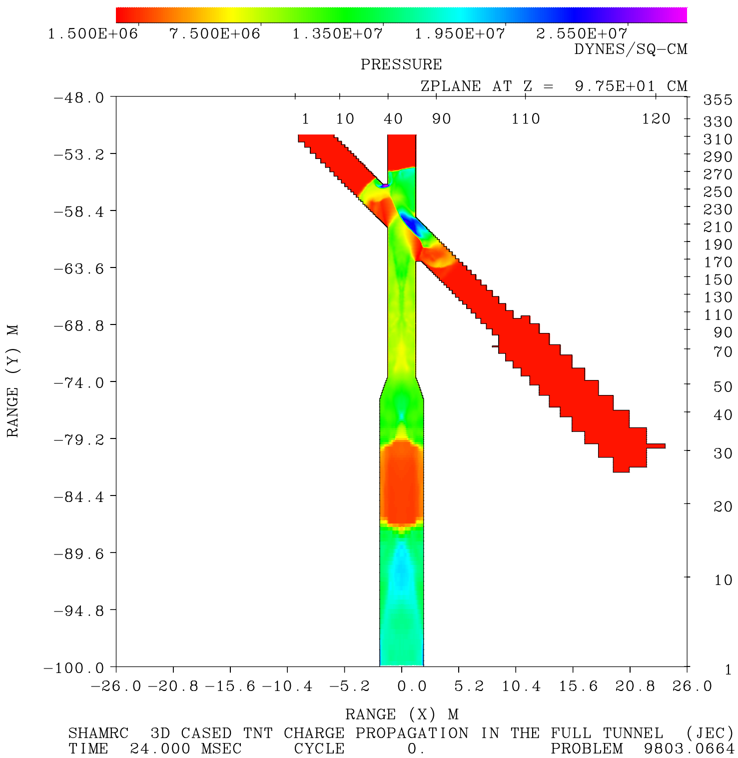

Figure 9 Pressure at 24 ms From Cased Charge Without Water

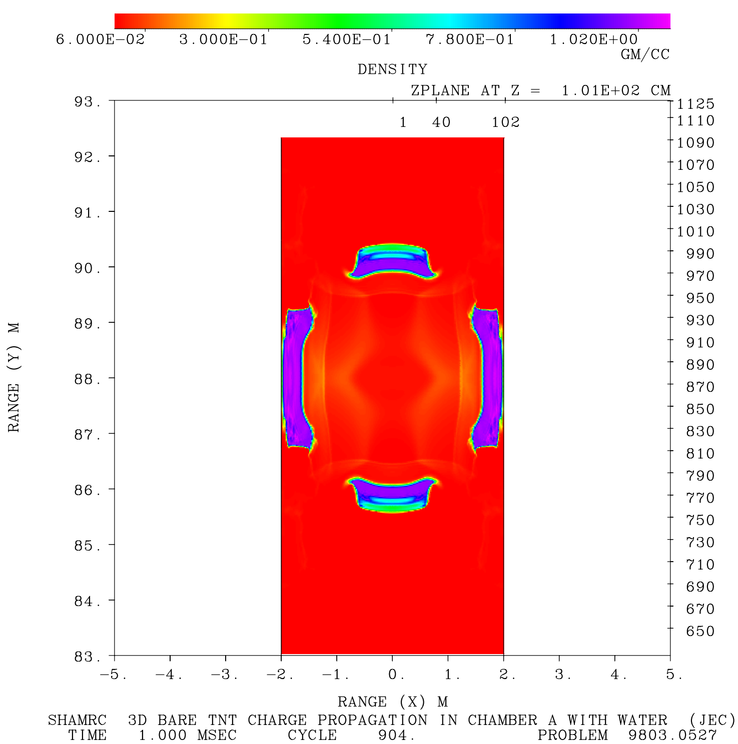

Figure 10 Density at 1 ms From Bare Charge With Water

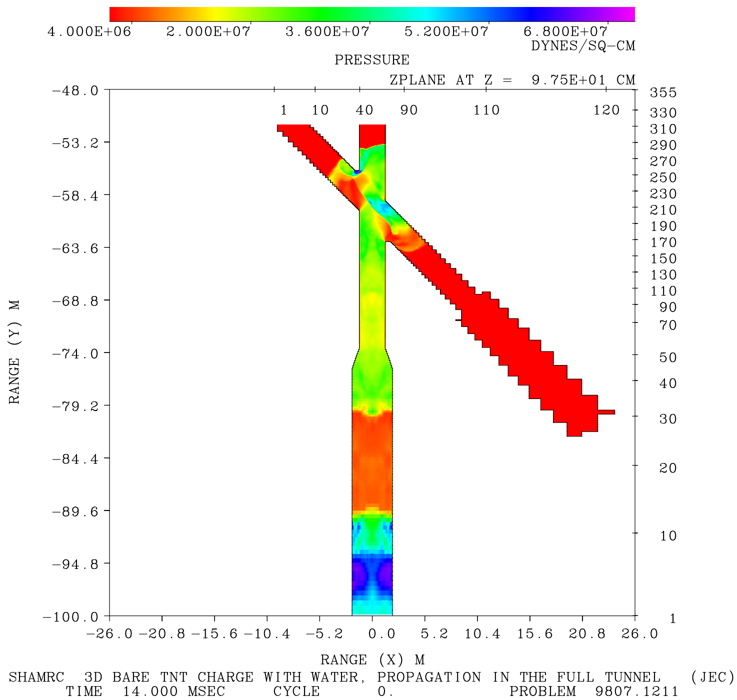

Figure 11 Pressure at 14 ms From Bare Charge With Water

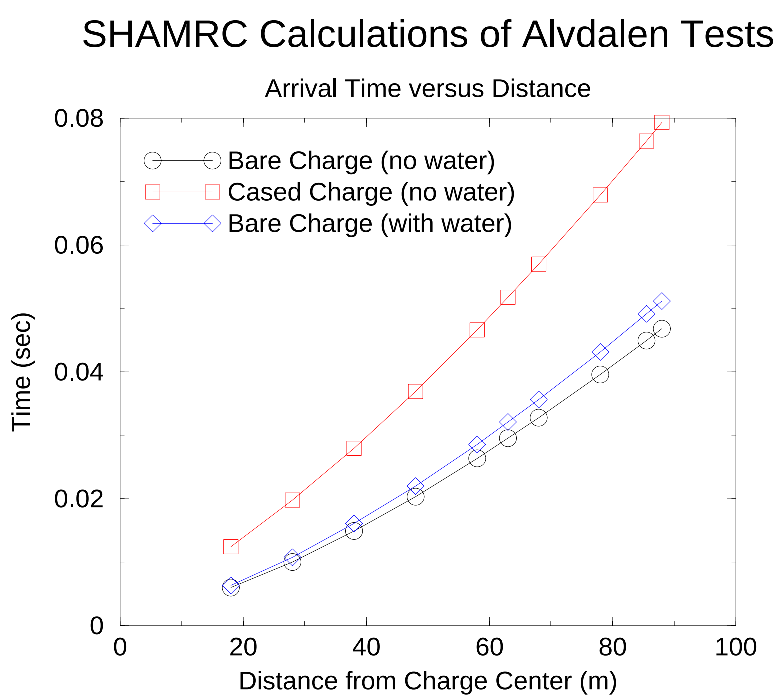

Figure 12 Arrival Time Comparison

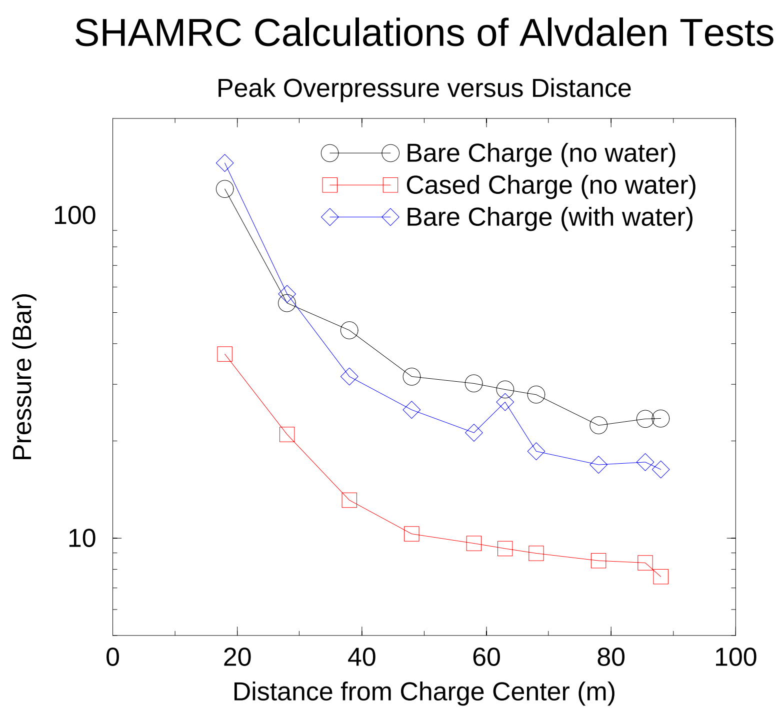

Figure 13 Peak Overpressure Comparison

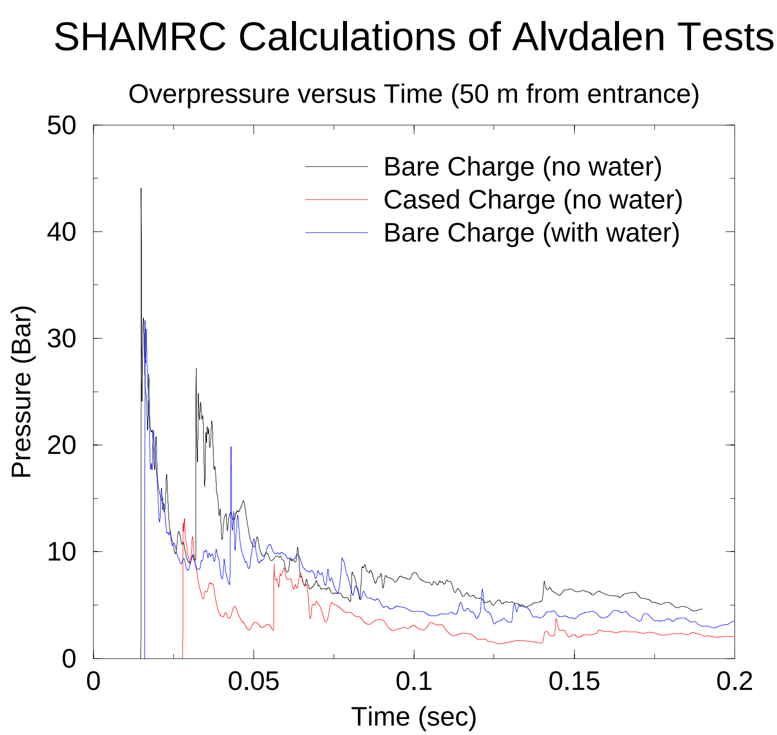

Figure 14 Calculated Overpressure-Time Histories 50 m From Tunnel Entrance

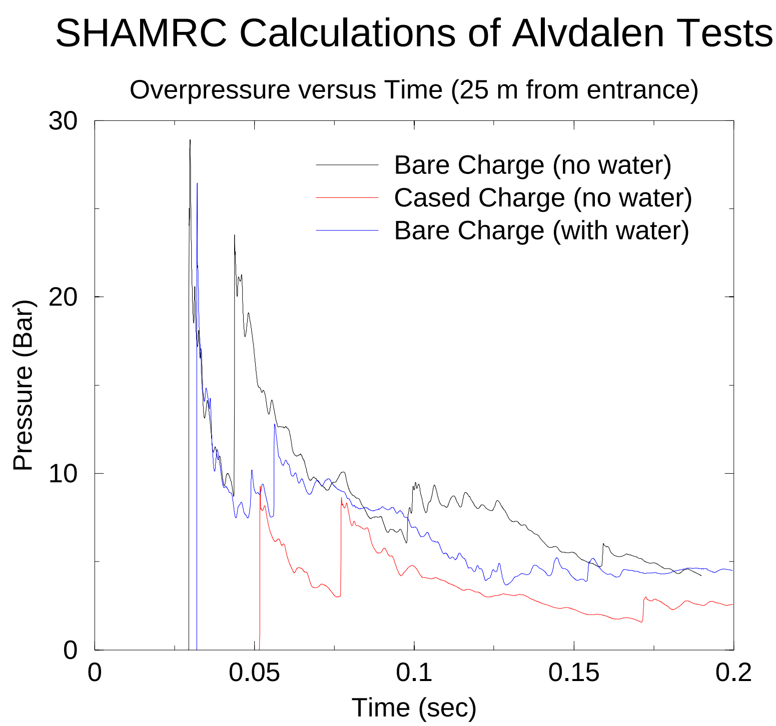

Figure 15 Calculated Overpressure-Time Histories 25 m From Tunnel Entrance

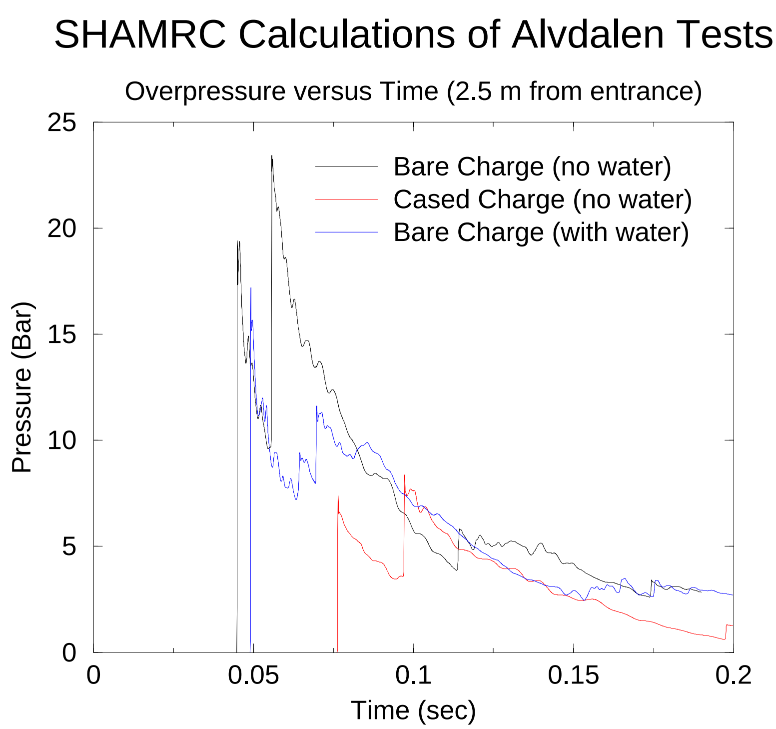

Figure 16 Calculated Overpressure-Time Histories 2.5 m From Tunnel Entrance

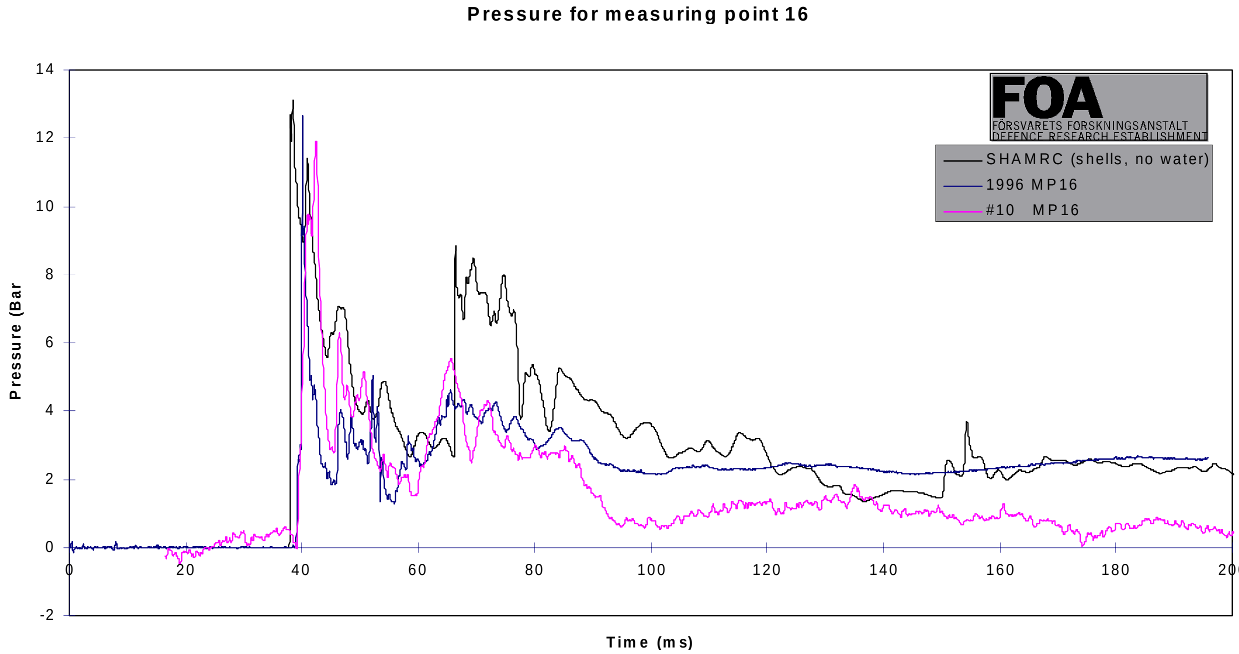

Figure 17 Overpressure-Time Histories 50 m From Tunnel Entrance

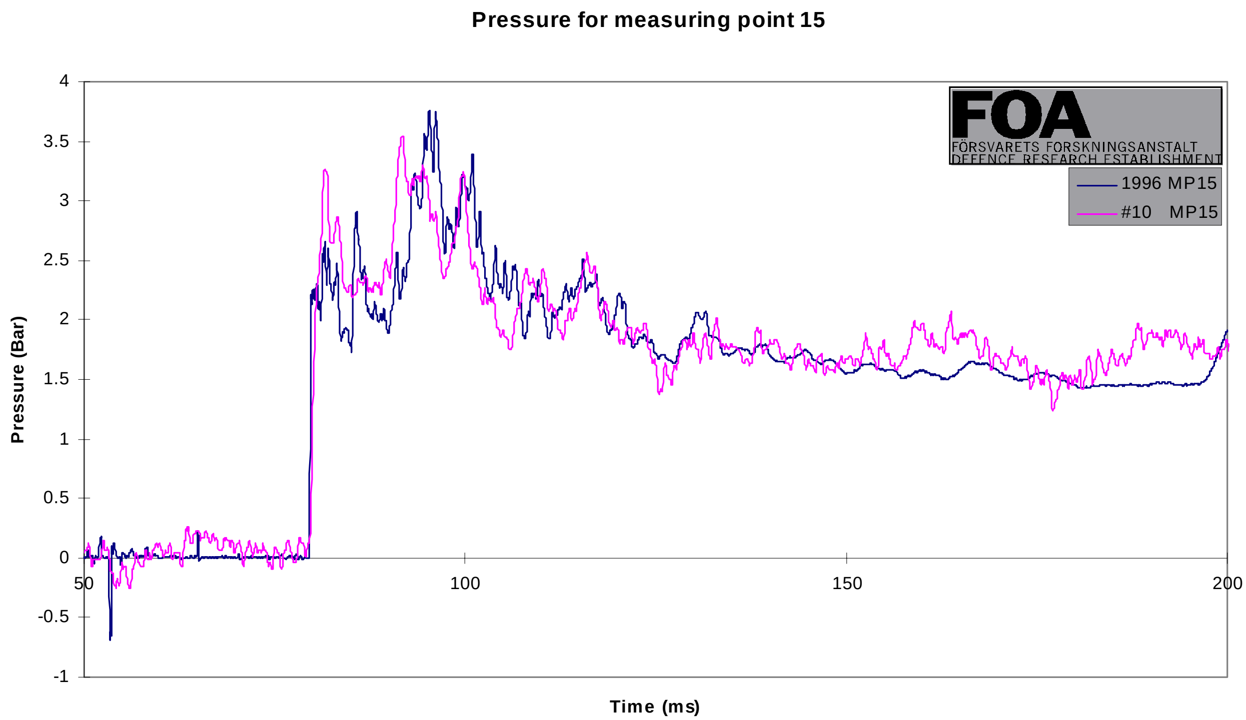

Figure 18 Experimental Comparisons 25 m From Tunnel Entrance

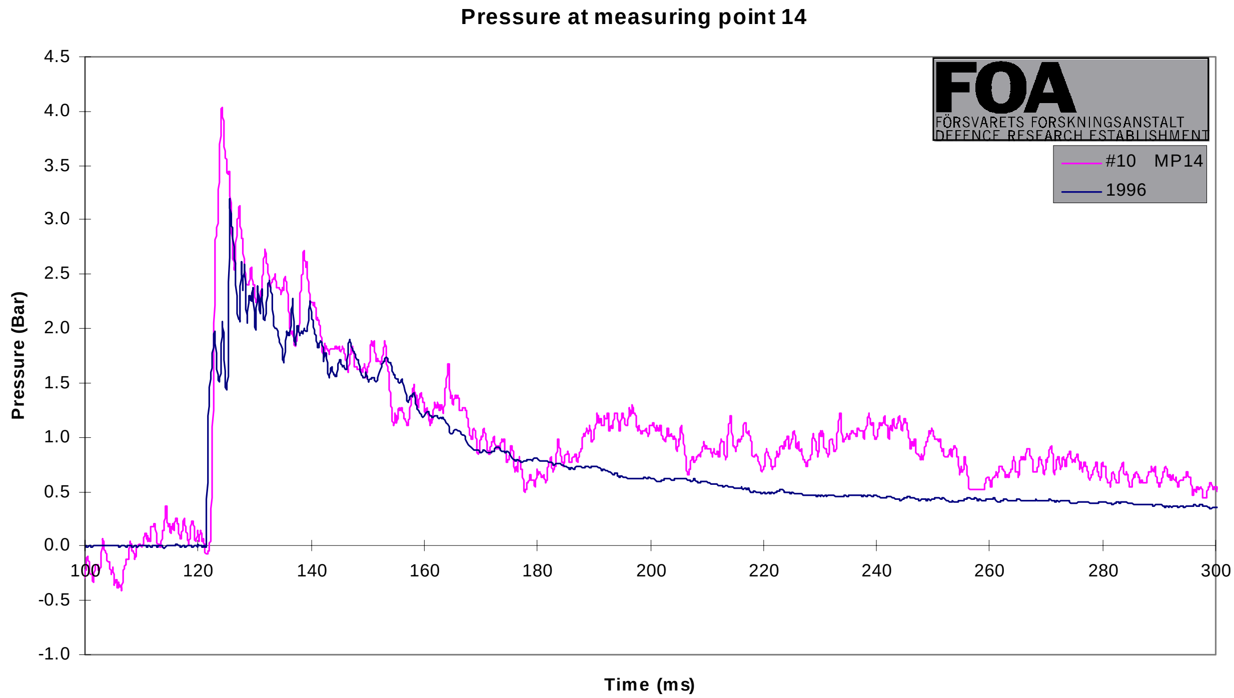

Figure 19 Experimental Comparisons 2.5 m From Tunnel Entrance